

Supporting Information:

SERS of Individual Nanoparticles on a Mirror: Size Does Matter, but so Does Shape

Felix Benz, Rohit Chikkaraddy, Andrew Salmon, Hamid Ohadi, Bart de Nijs, Jan Mertens, Cloudy Carnegie, Richard W. Bowman, Jeremy J. Baumberg*

NanoPhotonics Centre, Cavendish Laboratory, Department of Physics, JJ Thompson Ave, University of Cambridge, Cambridge, CB3 0HE, UK

*Correspondence and requests for materials should be addressed to jjb12@cam.ac.uk

S1. Size distributions of the nanoparticle samples used

The size distributions were determined by measuring the size of 150 particles from scanning electron microscopy (SEM) images. The extracted distribution curves are shown in Fig. S1.

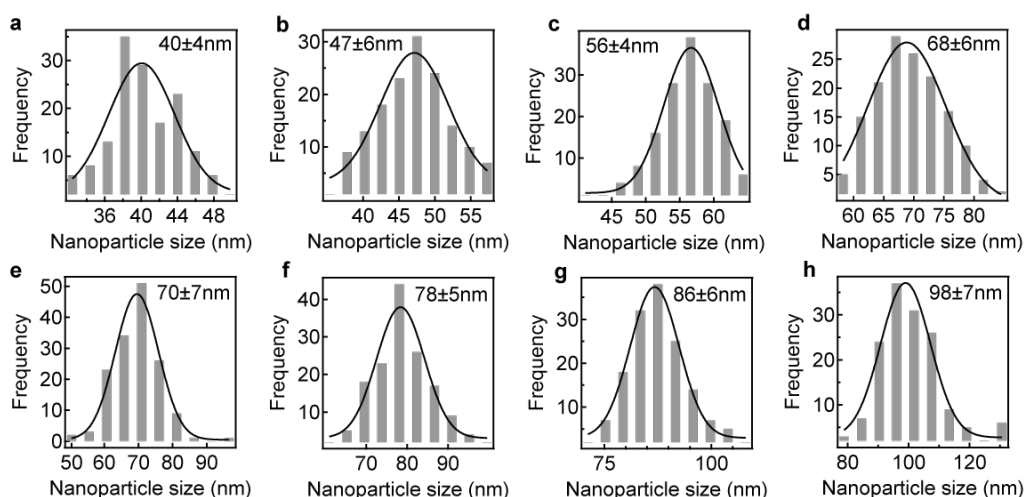


Figure S1. a-h, Nanoparticle size distributions for the nanoparticle samples. Determined from SEM images (see main text Fig. 1) for 150 particles per sample.

S2. FDTD results showing near- and far-field results for different nanoparticle sizes

The calculated scattering and near-field spectra for nanoparticles on a mirror with different nanoparticle sizes are shown in Fig. S2a, b. Figure S2c shows the increase of the scattering and near-field intensity with increasing nanoparticle size. The scattering response matches the experimentally observed r^6 dependence. The SERS scaling is weaker than that of the scattering, even though both involve an in-coupling ($\propto r^3$) and an out-coupling ($\propto r^3$). This is caused by the fact that while the scattering is mainly due to the radiative mode, the near-field on the other hand is composed of both radiative and non-radiative modes. Larger nanoparticles give rise to more non-radiative higher order

modes. Putting more weight on these modes reduces the weight of the radiative (antenna) mode. This discrepancy between near- and far-field is shown in Fig. S2d, which shows that the ratio of quadrupolar (see arrow) and dipolar mode are different for scattering and near-field.

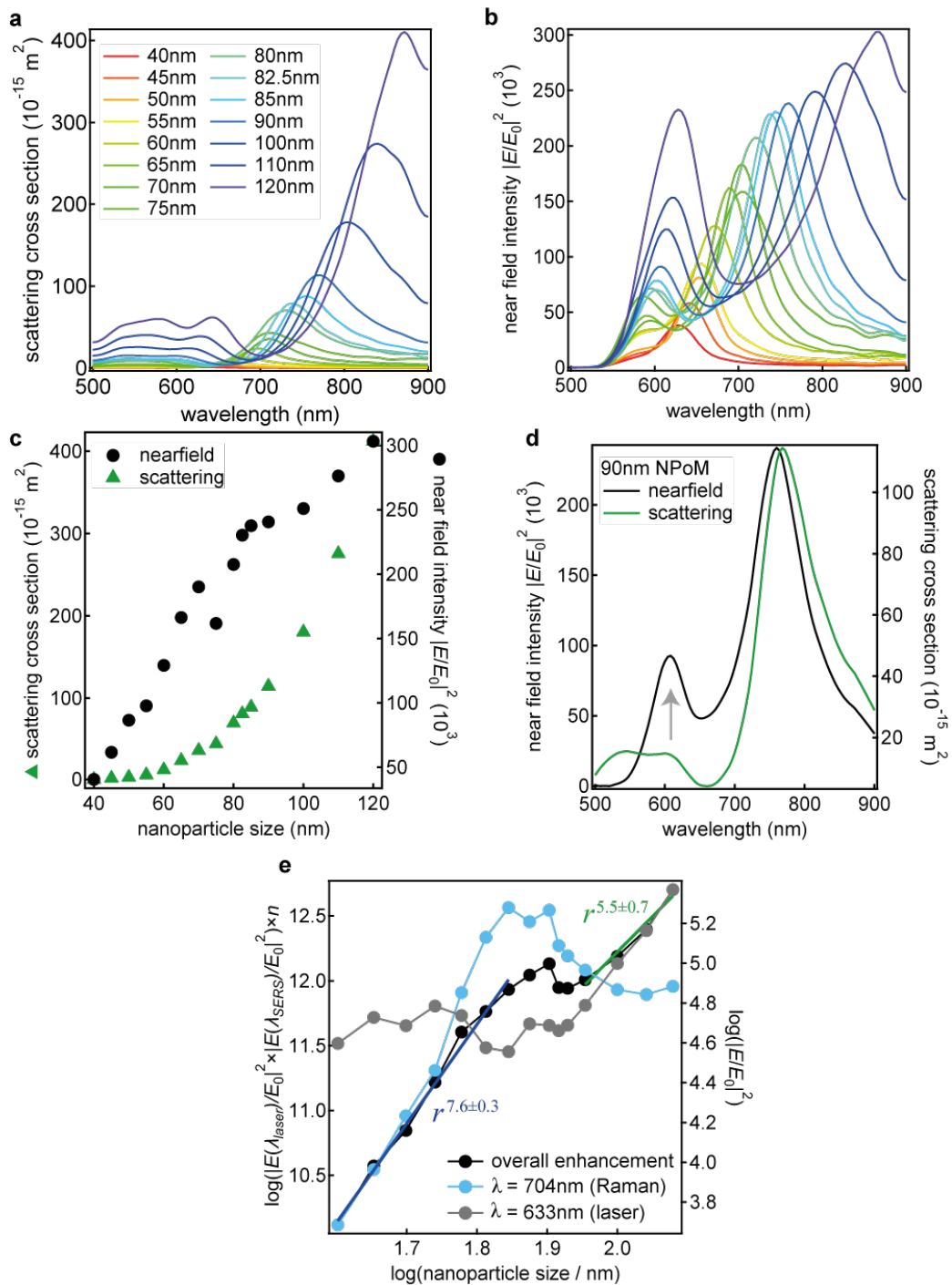


Figure S2. FDTD results for different nanoparticle sizes (spherical particles). **a&b**, Scattering and near-field spectra for different nanoparticle sizes. **c**, Extracted maximum near- and far-field intensity demonstrating power law scaling for the scattering. **d**, Comparison of scattering and near-field spectrum. **e**, Extracted SERS intensity for different nanoparticle sizes.

S3. Characterisation of the roughness of the gold film

The roughness of the gold films was measured using atomic force microscopy (AFM). Figure S3 shows the AFM image of a representative area on a template stripped gold film. The RMS roughness was determined to be 0.23 nm. Using such smooth gold helps to exclude additional effects due to the roughness of the gold film (usually present for slowly evaporated gold RMS roughness > 1 nm).

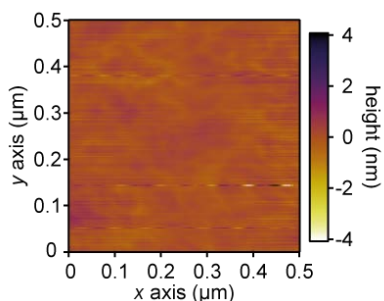


Figure S3. AFM image of a template stripped gold film. The RMS roughness was determined to be 0.23 nm.

S4. SERS data for additional BPT modes

Figure S4 shows the dependence of the SERS intensity on the BDP resonance wavelength for two additional Raman modes at 1075 cm^{-1} and 1278 cm^{-1} . The trend is similar to the one shown in the main text for the main Raman mode, showing an increased SERS response for larger nanoparticles (larger BDP resonance wavelength).

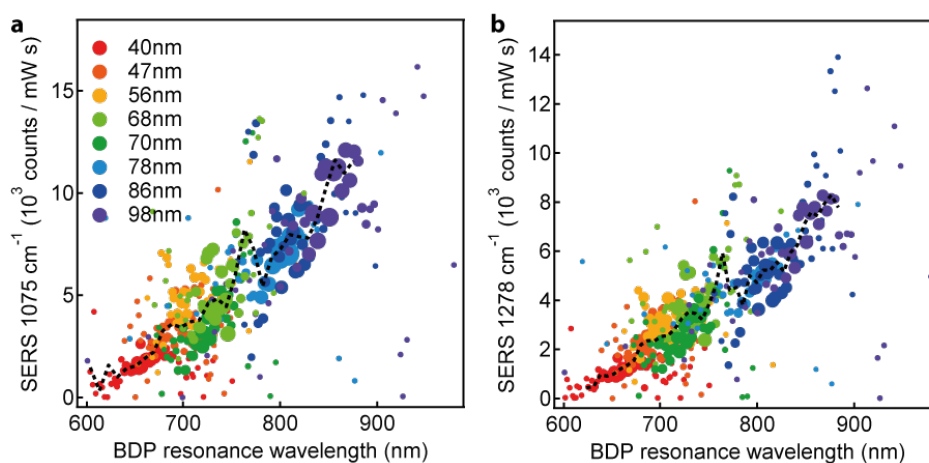


Figure S4. SERS intensity as a function of the BDP resonance wavelength for over 10,000 single nanoparticles. For clarity the single points are binned, and marker size gives number of single spectra per bin. **a**, 1075 cm^{-1} and **b**, 1278 cm^{-1} .

S5. Correlation with scanning electron microscopy

To confirm that all investigated spots are individual nanoparticles we have correlated dark-field scattering, SERS, and scanning electron microscopy (SEM) for several nanoparticles. The optical experiments were always performed first, as we found that SEM damages the molecular spacer layer. We note that these experiments are not performed on template stripped gold as a) the insulating glue layer between gold and silicon leads to charging effects and b) the electron beam damages the glue layer and therefore causes a huge amount of amorphous carbon deposition. Instead we use a gold film that was evaporated on silicon with a rate of 0.1 Å/s (using a 5nm thick adhesive chromium layer in between).

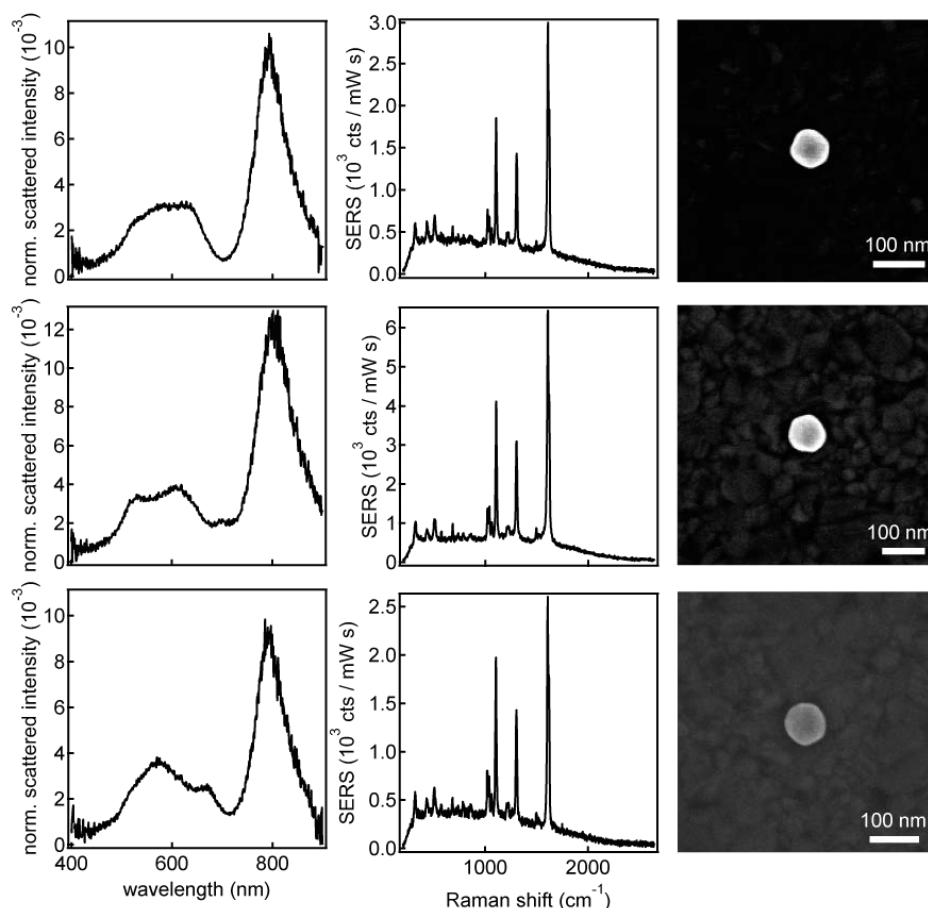


Figure S5. Correlation of dark-field scattering, SERS, and scanning electron microscopy for three different nanoparticles.

S6. Correction factor for scattering at larger angles

The scattering contribution of longer wavelengths is underestimated as the optical elements of the microscope are not optimised for wavelengths > 700 nm at high angles. This is particularly true for the coupled mode in the nanoparticle on mirror geometry which is emitted at an angle of approximately 58° . To compensate we record a calibration curve for emission under such a high angle. To do this we use the reflection from a $49 \mu\text{m}$ glass sphere (shown in the inset of Fig. S6b). We use dark-field illumination under an angle of approx. 55° and change the angle under which the light is reflected by changing the focus of the microscope (see illustration shown in Fig. S6a). The correction factor (Fig. S6c) shows that scattering at high angles in the NIR are underestimated by a factor of approx. 2. This correction is taken into account for the analysis of the scattering response shown in Fig. 3d (main text).

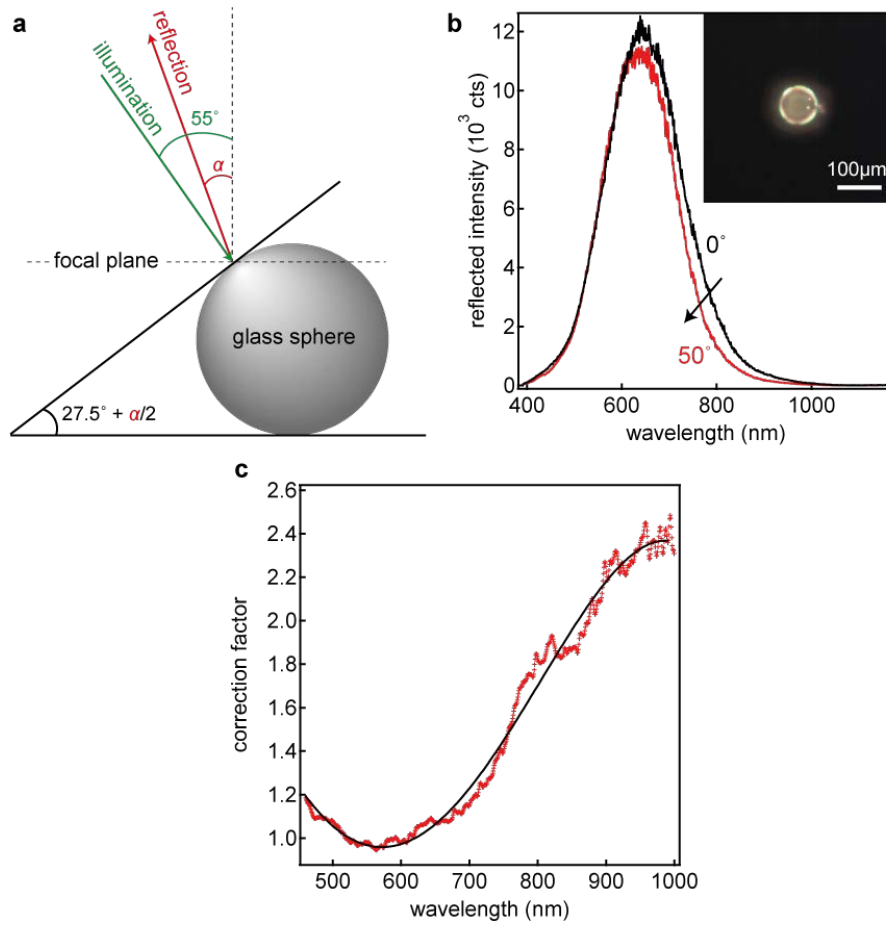


Figure S6. Correction factor for scattering at large angles. **a**, Illustration of the used geometry: light is reflected from a glass sphere at different angles depending on the position of the focal plane (local curvature). **b**, Example spectra for different reflected angles, the inset shows a dark-field image of the glass sphere. **c**, Wavelength dependent correction factor for scattering at 50° .

S7. Reduction of the near-field intensity due to faceting

As discussed in the main text, a faceted nanoparticle will have a lower near-field enhancement as the field is distributed over a larger area. To illustrate this effect Fig. S7a shows simulated near-field spectra for 80nm nanoparticles on mirror with different facet diameter. In order to compensate for the changing volume we have increased the radius of the sphere to keep the volume constant (for a constant radius, the decrease would even be more drastic). Extracting the expected Raman enhancement in terms of the field enhancement at the laser and Raman wavelength shows a strong decrease with increasing facet size.

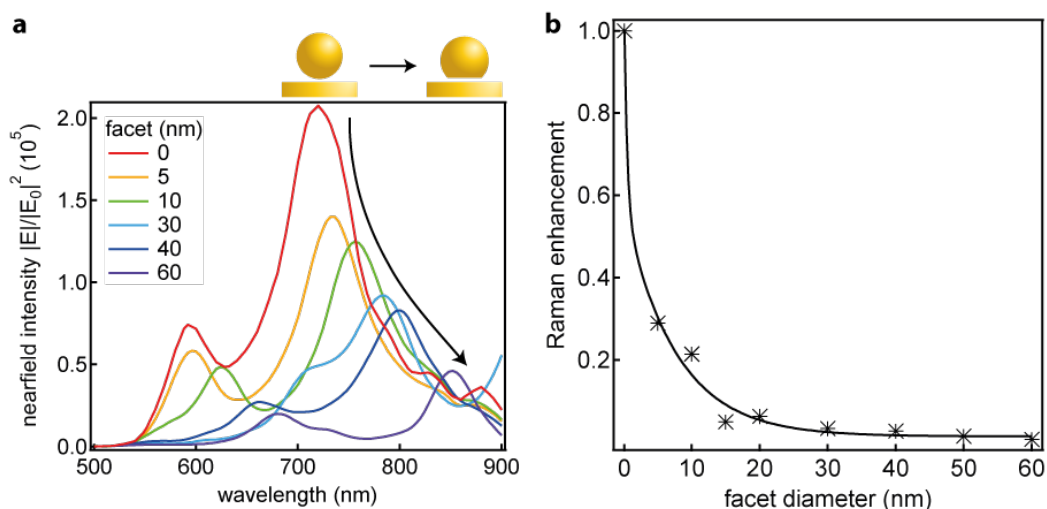


Figure S7. Influence of a growing facet on the field enhancement. **a**, Near-field spectra for different facet sizes, showing the decreasing intensity of both the dipolar and quadrupolar modes. All used particles have the same volume which is equal to the volume of a sphere with a diameter of 80 nm. **b**, Normalised reduction of the expected Raman enhancement as the facet diameter is increased.

S8. Distribution of observed resonance positions

Figure S8 shows an example of the distributions of resonance positions, FWHMs, and scattered intensities obtained for 98 nm nanoparticles (sample h, see section S1).

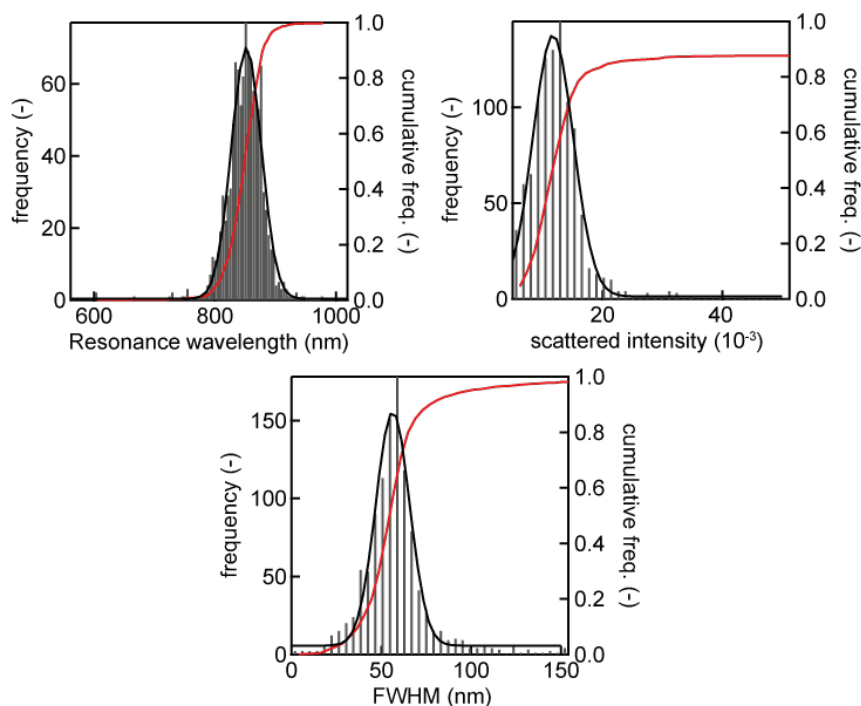


Figure S8. Distribution curves of the resonance wavelength, scattered intensity, and plasmon FWHM obtained by automated dark-field microscopy.